Earthquakes and Structures, *Vol. 11, No. 1 (2016) 109-127*
DOI: http://dx.doi.org/10.12989/eas.2016.11.1.109

Sensitivity analysis of probabilistic seismic behaviour of wood frame buildings

Jianzhong Gu*

Architectural and Engineering Technology, Thompson Rivers University, 900 McGill Rd, Kamloops, BC, Canada

(Received March 21, 2016, Revised May 20, 2016, Accepted June 23, 2016)

Abstract. This paper examines the contribution of three sources of uncertainties to probabilistic seismic behaviour of wood frame buildings, including ground motions, intensity and seismic mass. This sensitivity analysis is performed using three methods, including the traditional method based on the conditional distributions of ground motions at given intensity measures, a method using the summation of conditional distributions at given ground motion records, and the Monte Carlo simulation. FEMA P-695 ground motions and its scaling methods are used in the analysis. Two archetype buildings are used in the sensitivity analysis, including a two-storey building and a four-storey building. The results of these analyses indicate that using data-fitting techniques to obtain probability distributions may cause some errors. Linear interpolation combined with data-fitting technique may be employed to improve the accuracy of the calculated exceeding probability. The procedures can be used to quantify the risk of wood frame buildings in seismic events and to calibrate seismic design provisions towards design code improvement.

Keywords: earthquake engineering; probability; reliability; wood frame structures; timber; seismic effect

1. Introduction

Wood frame construction is the most commonly-used structural form in low-rise residential construction. Traditionally, wood frame buildings are believed to perform well in terms of life safety and collapse prevention during large earthquakes. However, significant damages and economic losses have been observed after several past earthquakes, such as the 1994 Northridge earthquake. As a result, the public's confidence towards seismic performance of wood frame buildings has been somewhat eroded. In some earthquake-prone regions, insurance premiums are significantly higher and unaffordable for many home owners. With increasing concerns to build earthquake resilience communities and build taller wood buildings, further understanding of seismic probabilistic behaviour of such structures will benefit stakeholders, builders, designers and homeowners.

Numerous studies on seismic reliability analysis of wood-frame structures are available. Ceccotti and Foschi (1999) used nonlinear dynamic analysis and first-order reliability methods to

*Corresponding author, Senior Lecturer, E-mail: jgu@tru.ca

http://www.techno-press.com/journals/eas&subpage=7 ISSN: 2092-7614 (Print), 2092-7622 (Online)

study a seismic design factor in the National Building Code of Canada. Rosowsky (2002) developed a risk-based methodology for seismic design of wood shear walls. A sequence of sensitivity studies was conducted to evaluate the contributions of various sources of uncertainty to shear wall performance using the CASHEW program (Folz and Filiatrault 2001). Zhang and Foschi (2004) reported their work in performance-based seismic design and reliability analysis using optimization methods to deal with the databases of structural response. The designed experiments and neural networks were implemented to improve computational efficiency. Wang and Foliente (2006) assessed the reliability of two low-rise non-symmetric wood frame buildings. It was found that uncertainties due to ground motion and structural modelling are the major sources for increases in estimated structural demand. Coupling of torsion and bidirectional excitation also causes significant response magnification. Pang *et al*. (2009) performed seismic fragility analysis of conventional one- and two-storey wood frame buildings in the central United States considering three failure mechanisms. Capacity, demand and modelling uncertainties were accounted for explicitly in the fragility analyses. Retrofit strategies were also suggested. Li *et al*. (2010) summarized collapse fragilities in different regions of the United States that account for differences in construction practices and site-specific seismic hazard. Their results suggested that current seismic design requirements in ASCE Standard 7-05 do not lead to uniform risk and may need to be revised. Pei *et al*. (2012) calibrated the response modification factor for a 6-storey cross laminated timber building. The calibration is based on an 80% probability of not exceeding 4% peak inter-storey drift during a maximum credible earthquake near Los Angeles, California, USA. van de Lindt *et al*. (2013) reported the development of a performance-based seismic design (PBSD) philosophy for midrise wood frame buildings and its validation. They examined the progress, current state, and challenges for PBSD of midrise wood frame buildings.

The objective of this paper is to present a discussion of sensitivity analysis to study seismic reliability of wood frame buildings. The CASHEW and SAWS programs (Folz and Filiatrault 2001, Folz and Filiatrault 2004) were used as a tool for nonlinear dynamic analysis. Two archetype buildings were studied in the analysis, a two-storey house and a four-storey apartment building. In order to accurately quantify the marginal contribution of related factors, numerical procedures methods were employed. The variations of seismic weights, ground motion records and intensity measure were compared for their contributions. Two different types of probability distributions of intensity were also discussed. Based on the results of sensitivity analysis, some recommendations were made for future study on seismic probabilistic behaviour of wood frame structures.

2. Description of configurations of archetype buildings

Two buildings were used in the analysis. The first building is the two-storey wood frame house tested as a part of the CUREE-Caltech Woodframe project at UCSD (Fischer *et al*. 2001). This building has a footprint of 4.9 m×6.1 m and a storey height of 2.6 m (Fig. 1). The lateral force resistance system of the building relied on exterior walls. The walls along the short direction (i.e., the north-south direction) had large openings for doors and windows and thus were considered to be the weak direction. All exterior walls were sheathed with 9.5-mm thick oriented strand board (OSB) panels that fastened to the framing with 8-penny box gun nails. Tie-downs (Simpson Strong-tie HTT22) and steel straps (CS16) were used at all openings. 12-mm thick gypsum wallboard (GWB) panels were installed on the interior side with 32-mm long screws. A total thickness of 22 mm of stucco with 17-gauge galvanized steel wire lath was applied to the exterior

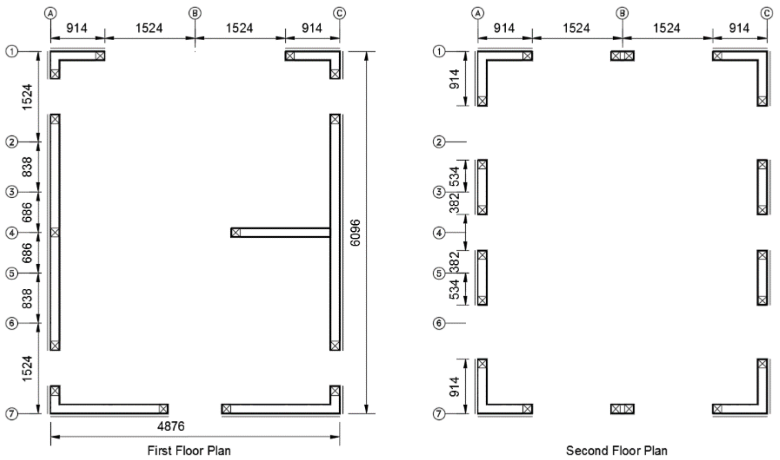

Fig. 1 Floor plan of the two-storey building

connected with 20-mm long staples. The locations and length of walls can be found in Fig. 1. Further details of this building can be found in the Phase 10 test of related publications (Fischer *et al*. 2001, Filiatrault and Folz 2002).

The second building is a four-storey apartment building, which represents typical multi-storey residential buildings on the west coast of North America (Fig. 2). The building had a footprint of 57.19 m×19.23 m and a uniform storey height of 2.79 m. There was a corridor in the middle along the longitudinal direction. The building has two stairs and 14 units, rotationally symmetric to the center of the floor plan. It had many windows and doors on the exterior side to maximize the view and day light. Thus, the lateral force resistance system of the building relied on five types of interior walls, which are indicated as "S.W." in Fig. 1. The spacing of wall studs were 405 mm. 9.5-mm OSB panels were used as sheathing panels and fastened to framing members with 65-mm spiral nails. Nails were spaced at 305 mm along the interior of the panels. Along panel edges, nail spacing vary from location to location, as shown in Table 1. It should be mentioned that typical "party" wall details apply to those between two adjacent units (i.e., S.W.1 and S.W.2). Each of these party walls had two nominal two-by-four walls side by side with a 25 mm gap in order to improve acoustic performance of the built environment. All shear walls were properly anchored by metal straps, tie-rods and/or other means to prevent uplift. Other walls were either partition walls or not properly detailed for lateral force resistance. Therefore all those walls were assumed not to contribute to the lateral stiffness or strength of the building. The floor assembly consists of GWB, nominal two-by-ten (38 mm×140 mm) joists, 12.5-mm OSB, 38-mm concrete topping and flooring finish, which weighs 2.0 kPa in average for the whole floor. The average seismic weight on the roof was 1.5 kPa.

These two buildings are intended to represent typical residential buildings in North America. Typical single-family residential buildings in this region are one or two storeys, the design of which follows prescriptive requirements in building codes. Many multi-family apartment buildings are traditionally four-storey wood frame structures, which need to be designed by engineers. The two-storey house is an example of non-engineered wood frame buildings. The design of such type of buildings is usually completed by one or two major designers, who have the control of both structural and non-structural elements. The CUREE house has been well-studied experimentally

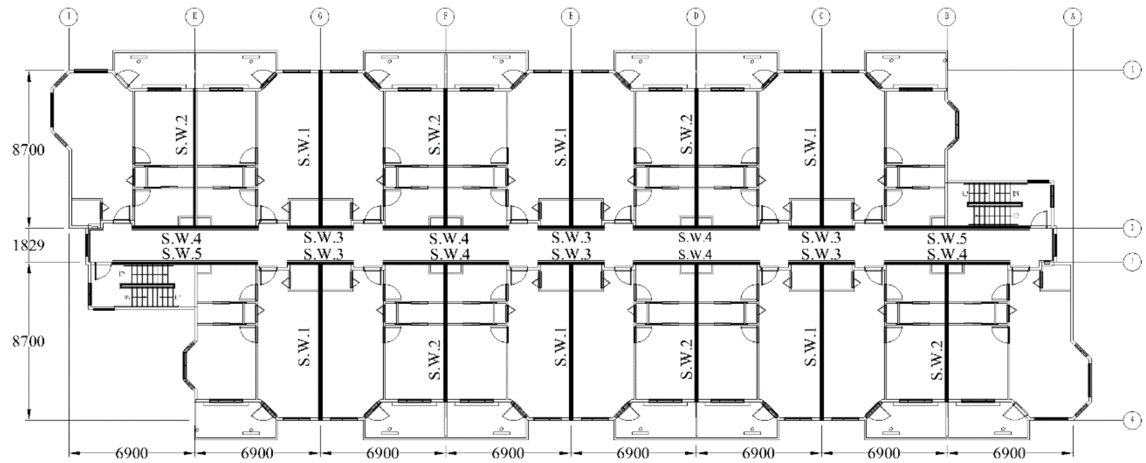

Fig. 2 Floor plan of the four-storey building

Table 1 The nailing schedule of the four-storey building

	S.W.1~2 (mm)	S.W. 3~5 (mm)
4th floor	150	150
3rd floor	150	150
2nd floor	150	100
1st floor	150	75

and analytically. Therefore, it is chosen to represent single-family buildings. The four-storey building is an example of engineered buildings. This building represents common practice of multi-family apartment buildings in this region. The primary structural engineers of engineered buildings are usually only responsible for major structural elements. The information of secondary and non-structural elements, such as the connections and openings of GWB panels, is not available for primary structural engineers at the time of structural design. Therefore, the contribution of GWB to lateral resistance was not considered in the four-storey building.

3. Shear wall model

The reversed cyclic behaviour of all shear walls was simulated with CASHEW (cyclic analysis of shear walls), a program that was developed by the CUREE-Caltech Woodframe project (Folz and Filiatrault 2001). The results of each wall obtained from CASHEW were used to calibrate the parameters of a single degree-of-freedom nonlinear hysteretic spring with strength and stiffness degradation. With these nonlinear springs, the numerical program SAWS (seismic analysis of woodframe structures) (Folz and Filiatrault 2004) was used to perform three-dimensional nonlinear analyses of the structures. The SAWS program is a pancake model using the assumptions of rigid diaphragms and zero-height nonlinear springs. Each shear wall is modeled as a nonlinear spring defined by the hysteresis model and placed at the center of the wall. The parameters of the springs are calibrated using search algorithms embedded in CASHEW. With the response of all springs and the rigid diaphragm, each floor is modeled as three degrees of freedom. Incremental dynamic analysis (IDA) (Vamvatsikos and Cornell 2002) was performed at different levels of intensity using SAWS. This program was incorporated into a Microsoft Excel spreadsheet using Visual Basic for iterative calculation and data visualization. The use of CASHEW and SAWS was based on the availability and computational efficiency of NTHA.

4. Reliability methods

4.1 Ground motion records and scaling method

A suite of 22 pairs of ordinary earthquake ground motion records by FEMA P-695 (ATC 2009) were used as the input for the nonlinear time-history analysis (NTHA). These ground motion records were scaled to multiple levels of intensity measure using a scaling method to account for the variation of earthquake loads. The probabilistic seismic behavior can be computed from the results of IDA with the selected ground motion records.

The scaling process involved three steps: i) the normalization, ii) the basic scaling and iii) the secondary scaling. The first two steps were promoted by FEMA P-695. During the normalization, all records were scaled to their median peak ground velocity. In the second step, all records were scaled to have a median spectral acceleration (S_a) to match the targeted spectral acceleration for the maximum considered earthquake (MCE) at the fundamental period. With the second step, the ground motion records were scaled to a deterministic level of intensity (i.e., the median spectral acceleration). To ensure a probabilistic analysis, the targeted intensity level should not be deterministic. The third step, secondary scaling, was used to consider the uncertainty of intensity measure for reliability analysis with the scaling factors dependent on the selected distribution types as discussed below.

4.2 Sources of uncertainties and their distributions

Three sources of uncertainties were considered in the sensitivity analysis: seismic weights, record-to-record variability, and intensity measure. Seismic weights mainly come from dead loads of structural and non-structural components. A lognormal distribution with a coefficient of variation (COV) of 0.1 was assumed for seismic weights of all floors and roofs. Generally, the seismic weights at different floors and roof can be assumed to be uncorrelated or having a correlation coefficient not significantly different from zero. However, uncorrelated seismic weights may produce some cases with significant vertical weight irregularities which is either not permitted by typical building codes or should be avoided by construction practice. It was also noted that the floor assembly is commonly the same for all levels. The materials for all levels were assumed to come from the same suppliers or perhaps even the same shipment. Thus, it would be reasonable to assume that seismic weights at different floor levels are highly correlated. It would be practical and reasonable for this paper to assume that the correlation coefficients between any two floors are equal to 1.

The annual occurrence probability of intensity measure, $H(\cdot)$, is traditionally assumed to be linear on a log-log plot, shown as

$$H(S_a) = aS_a^{-b} \tag{1}$$

where S_a=spectral acceleration; a and b are parameters. This assumption produces an extreme-type distribution for the targeted exceeding probability within the expected life time of the structures.

There is no doubt that such kinds of distributions are reasonable to describe the real occurrence probability of earthquakes for earth scientists. In terms of construction practice, most structures, if not all, have been designed or proved to resist certain levels of earthquakes. Engineers, architects and stakeholders may not be interested in the consequence to structures from small earthquakes. Rather, they may be more interested in the consequence from reasonably large earthquakes within the life period of structures. Their concerns to the performance at targeted intensity levels may be descripted by some questions such as “what is the consequence if a 8.0-magnitude earthquake hits this region”. Reliability analysis targeted at certain intensity levels may provide more information for disaster prediction and mitigation. In term of seismic reliability analysis, the extreme-type distributions produce many samples at low intensity levels. The demand calculated from these low-intensity samples may not exceed the threshold to contribute to damage or failure probabilities. Samples near targeted design intensity levels are scarce but useful for analysis. In order to address the concerns from construction practice and reliability analysis, the lognormal or other similar distributions with the mean near the targeted intensity levels may be employed. Such distribution types allow samples concentrating around the targeted intensity level. The variation for the distributions of intensity measure is used to consider the aleatoric and epistemic uncertainties associated with the targeted hazard. The probabilistic analysis conducted with this type of distribution may be viewed as an extension of the fragility analysis.

For comparison, both the extreme-type distribution shown in Eq. (1) and the lognormal distribution were used in the analysis of the two-storey building. Based on previous research (Li *et al*. 2010, Cornell *et al*. 2002, ATC 2009), the parameters a and b in Eq. (1) were chosen to be 0.0144 and 3.2, respectively. These numbers correspond to a targeted spectral acceleration of 0.9 g at the exceeding probability of 2% in 50 years. The basic scaling factor of the two-storey building was 1.93. The scaling factor for the second scaling is defined as the ratio of a sample of the distribution to the median spectral acceleration for the Seismic Design Category (SDC) of D_{max} defined in FEMA P-695. This case is referred to as “the extreme-type distribution”. Two lognormal distributions were also used. The mean value of the first lognormal distribution was set to the median spectral acceleration for the SDC of D_{max} in FEMA P-695. The COV was set to 0.3. The scaling factor for the second scaling is defined as the ratio of a random sample to the mean value of the distribution. This is the baseline case widely used in this paper unless noted otherwise. The second lognormal distribution had a mean value of 1.5 times of the median spectral acceleration and a COV of 0.3. This case is referred to as the “2nd lognormal distribution”. The four-storey building was assumed to have a lognormal distribution with a mean value equal to the median spectra acceleration for the SDC C_{max}-D_{min} in FEMA P-695 and a COV of 0.3. The basic scaling factor for the four-storey building was 0.80. This COV of 0.3 was chosen with the reference of typical live loads.

The selected ground motion records were implicitly assumed to be uniformly distributed over the range of its variation. All records contribute equally to the representative probability. Therefore, the distribution of the records can be expressed as a probability density function, $f_R(\cdot) = 1/N$, where N is the total number of selected ground motion records. The discrete form of the density function, $f_R(r_j)$, may be used instead of $f_R(r)$ in the following discussion. The uncertainties from other sources, such as structural configurations, have been well discussed by others (Pang *et al*. 2009, Li *et al*. 2010) and were not considered here.

4.3 Traditional reliability method

The traditional method estimates the exceeding probability of drift demand from conditional distributions given intensity levels, shown as

$$F_D(d) = P(D \le d) \approx \int_0^{+\infty} P[D(a) \le d | IM = x] f_{IM}(x) dx \tag{2}$$

where $P[D(a) \le d | IM = x]$ is the conditional cumulative distribution function (CDF) of drift demand, D, not exceeding the value d, given the intensity level of *IM*=*x*. This conditional distribution of drift demand, D, has the uncertainties from ground motion records, r, and resistance property, *a*. In this case, the uncertainty from seismic weights is the only resistance property.

Two ways may be employed to solve the problem with the uncertainty from seismic weights and other sources. One way is to use the approximate conditional distribution to further simplify Eq. (2) shown as

$$F_D(d) = P(D \le d) \approx \int_0^{+\infty} \{ \int_{-\infty}^{+\infty} P[D \le y | (A = a, IM = x)] f_A(a) da \} f_{IM}(x) dx \tag{3}$$

where the conditional distribution, $P[D \le y | (A = a\ , IM = x)]$, is established by ranking the results of drift demand from all ground motion records, conditioned on resistance property, *a* and intensity measure, *x*. If two or more resistance uncertainties are considered, double or multiple integrals will be used for the conditional distribution, $P[D \le y | (A = a\ , IM = x)]$.

The other way to obtain the exceeding probability, $P[D(a) \le d | IM = x]$, is to rank the results by sampling the probability domain of seismic weights. Then NTHA is performed for structures with different seismic weights for all ground motion records at the intensity level of *IM*=*x*. Ranking the drift demand from all NTHA produces the conditional distribution of $P[D(a) \le y | IM = x]$. Actually, this is using Monte Carlo simulation (MCS) locally considering the uncertainties from records and seismic weights. The results from the simulation may be more accurate than that shown in Eq. (3), as the simulation determines the conditional distribution directly.

With the probability density function of capacity, $f_C(y)$, the probability of failure in Eq. (2) may be expressed as

$$\begin{aligned} P_f &= \int_0^{+\infty} f_C(y)[1 - F_D(y)] dy \\ &\approx \int_0^{+\infty} f_C(y)\{1 - \int_0^{+\infty} P[D(a) \le y | IM = x] f_{IM}(x) dx\} dy \end{aligned} \tag{4}$$

Considering the nature of NTHA, a closed-form solution to Eqs. (2) or (3) may not exist. A numerical format of Eq. (4) used in this study is expressed as

$$P_f = \sum_{k=0}^{L} f_C(y_k)\{1 - \sum_{i=0}^{M} P[D(a) \le y | IM = x_i] f_{IM}(x_i) \Delta x_i\} \Delta y_k \tag{5}$$

where M is the number of intensity levels and L is the number of capacity levels. The discrete samples of seismic weight have been incorporated in the conditional CDF.

The conditional probability distributions, $P[D(a) \le y | IM = x]$, with uncertainties from ground motion records and seismic weights were used to compare the influence of different factors. The comparison produces multiple probability distribution curves at different levels of intensity at *IM*=*x*.

4.4 A method based on conditional distributions at given ground motion records

The conditional probability distributions of drift demand in Eq. (2) are constructed from all records at given intensity levels. Similarly, the conditional distributions of drift demand can be constructed from intensity measure at given ground motion records. Then the exceeding probability of drift demand can be established as

$$F_D(d) = P(D \le d) \approx \int_0^{+\infty} P[D(a) \le d \,|\, R = r]\, f_R(r) dr \tag{5}$$

where $P[D(a) \le d \,|\, R = r]$ is the conditional CDF of drift demand not exceeding the value d, considering the uncertainties from intensity measure and seismic weights, given the ground motion record of R=r. The integral sign in Eq. (5) means that the variable, r, for ground motion records is expected to be continuous. Since the ground motion records are always discrete samples representing their earthquake characteristics, a practical form of Eq. (5) is shown as

$$F_D(d) = P(D \le d) \approx \sum_{j=1}^{N} P[D(a) \le d \,|\, R = r_j]\, f_R(r_j) \Delta r_j \tag{6}$$

Here j denotes the j^{th} ground motion record under consideration. Since the selected ground motion records are uniformly distributed in their representing ground motion characteristics, the values of the probability density function, $f_R(r_j)$, for all records are the same. The intervals between a pair of adjacent ground motion records, Δr_j, are also the same. Therefore, one has

$$f_R(r_j)\Delta r_j = \frac{1}{N} \quad (j = 1, 2, \ldots, N) \tag{7}$$

Substituting Eq. (7) into Eq. (6) gives

$$F_D(d) \approx \frac{1}{N} \sum_{j=1}^{N} P[D(a) \le d \,|\, R = r_j] \tag{8}$$

The probability of failure can be expressed as

$$\begin{aligned} P_f &= P(C < D) = \int_0^{+\infty} f_C(y)\{1 - F_D(y)\} dy \\ &\approx \sum_{k=0}^{L} f_C(y_k)\{1 - \frac{1}{N} \sum_{j=1}^{N} P[D(a) \le y_k \,|\, R = r_j]\} \Delta y_k \end{aligned} \tag{9}$$

The probability of structural failure expressed in Eq. (9) is determined from the mean of the conditional exceeding probabilities of drift demand over selected earthquake records. The conditional probability function, $P[D(a) \le y_k | R = r_j]$, is established from the IDA curves of all possible structural configurations for the j^{th} ground motion record. The randomness of the conditional exceeding probability comes from both intensity measure and resistance property. Similar to the traditional method (Eq. (2)), the conditional distribution in Eq. (9) can be solved from a double integral of conditional distributions. It also can be solved using a localized MCS by ranking the drift demand from NTHA considering uncertainties from intensity and seismic weights. This method will be referred to as the second method.

The conditional probability distributions, $P[D(a) \le y_k | R = r_j]$, with uncertainties from intensity measure and seismic weights were used to compare the influence of different factors. Each ground motion records has a single conditional distribution.

4.5 The Monte Carlo simulation and sampling strategies

The probability distribution of ground motion records can be considered as a uniform distribution. Each record is a natural sample representing ground motion characteristics. The distribution of intensity and seismic weights can be defined from statistical data. Therefore, the drift demand follows a joint probability distribution of resistance, records and intensity. If other uncertainty sources are considered, the joint distribution will have more random variables. Compared with the two methods discussed above, the MCS method may be used as a benchmark to account for the uncertainties from different sources.

The computational demand of the classic MCS using pseudo random numbers is significant due to the time-consuming process of NTHA. However, the quasi-Monte Carlo simulation with sequence samples can be used to reduce the number of samples and thus improve the computational efficiency.

Different combinations of sample numbers were used to investigate their influences. A preliminary calculation used 40 samples for intensity and 16 samples for seismic weights, following the technique for quasi-Monte Carlo simulation. With 22 samples of ground motion records (i.e., 22 pairs of records), the preliminary calculation ran NTHA for 14080 times. Then 22 pairs of records were rotated by 90 degree and NTHA is repeated. After the preliminary calculation, the sample number of seismic weights was reduced to 8, 4 or 1. One sample implies that the mean value was used in the calculation and no variation was considered. In the discussion below, the term of “fixed weights” was used instead of “one sample”. Meanwhile, the sample of intensity was reduced to 20 or 10. The combinations of different sample numbers for intensity and seismic weight were studied using the MCS method as well as the methods discussed above.

5. Results and summary

5.1 Sensitivity analysis with the traditional method for the two-storey building

The numerical procedures for the three methods discussed above do not use any data fitting technique, if data points are sufficient. These numerical procedures have the advantage of retaining the accuracy of results from NTHA for reliability analysis. With these procedures, the influences of different factors and sources of uncertainties can be accurately quantified and compared for their contributions.

Three questions were examined for the influences of seismic weights. The first question was the contribution of uncertainty from seismic weights, relative to that from ground motion records and intensity. The second question was the influence of sample sizes for seismic weights and intensity measure and to identify the optimized sample sizes. The third question was how well the distribution curves can fit certain distribution types such as the lognormal distribution.

The conditional distribution, $P[D(a) \le y | IM = x]$, as illustrated in the traditional method was obtained at up to 40 levels of intensity for the two-storey building (Fig. 3). Each curve consists of 22 data points from 22 records, which may be not sufficient to accurately describe the tail of the probability distribution. The advantage of the traditional method is that sampling strategy for intensity can be arbitrary. Fig. 4 shows a comparison extracted from Fig. 3 at three levels of spectral acceleration: 0.671 g, 0.915 g and 1.21 g. In these figures, "fixed weights" means that no variation was considered for seismic weights. Simply speaking, "fixed weights" is a fragility curve with the only uncertainty from ground motion records. "Variable weights (8 samples)" means that eight samples were taken from the distribution of seismic weights. With 22 records (or samples), a curve for "variable weights (8 samples)" consists of 176 data points. Similarly, a curve for "variable weights (16 samples)" has 16 samples for seismic weights and consists of 352 data points.

Generally, the probability distribution curves at three levels of spectral acceleration (Fig. 4) show similar results. The results for "fixed weights" do not significantly deviate from the curve of "variable weights (16 samples)" except for some records. This may be further explained that the drift from NTHA is not very sensitive to the variation of the seismic weight. The variation of seismic weights does not play a significant role compared with ground motion records (Fig. 4(a)). It is also shown that the fragility curve for "fixed weight" has limited data points and may not produce an accurate result for the tail of the distribution. The samples from seismic weights appear to produce more data points and result in a smooth probability distribution curve. The curves for "variable weights (8 samples)" and "variable weights (16 samples)" do not show much difference, which implies that 8 samples are sufficient to produce smooth conditional distribution curves for the traditional method. Other calculations showed that the sample number of seismic weights may not be further reduced to 4 or 5 samples.

The data curves for variable weights with 16 samples were fit with lognormal distributions using the maximum likelihood estimation. The original curves and fitted lognormal distributions were compared with some examples shown in Fig. 4. From this comparison, it can conclude that the accuracy of fitted lognormal distribution totally depends on the design point. Some accuracy will be lost if fitted lognormal distributions are used in reliability analysis.

5.2 Sensitivity analysis with the second method for the two-storey building

The conditional probability distributions, $P[D(a) \le y_k | R = r_j]$, as illustrated in the second method was obtained at 22 pairs of ground motion records (Fig. 5). Fig. 5(a) shows the results without

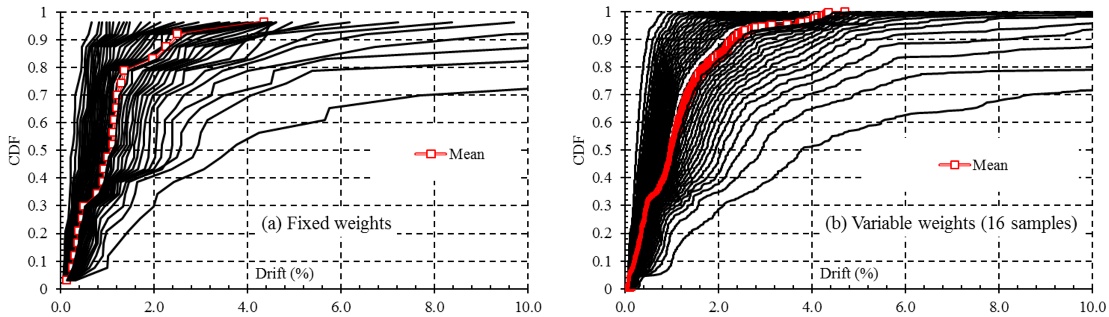

Fig. 3 Conditional distributions at 40 levels of intensity for the traditional method

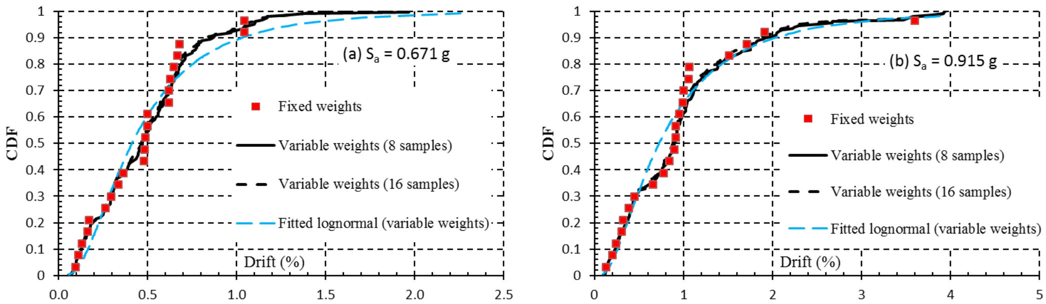

Fig. 4 Comparison of conditional probability distributions for the traditional method

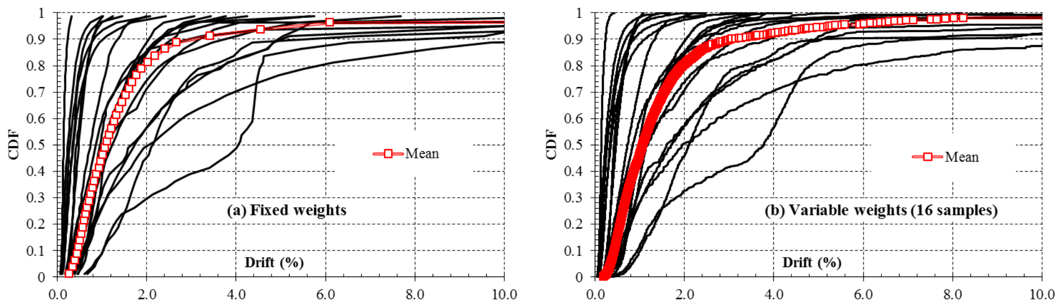

Fig. 5 Conditional distributions at 22 pairs of records for the second method

considering the uncertainty from seismic weights. Each curve in Fig. 5(a) has 40 data points at the selected 40 levels of spectral acceleration. Compared with Fig. 3(a), the distribution curves in Fig. 5(a) can be very accurate in the tail by increasing the number of samples of intensity measure or using different sampling strategies. Fig. 5(b) shows the conditional distributions considering the uncertainties from both intensity and seismic weights. 16 samples were used for the uncertainty of seismic weights, which result 640 data points for each curve in Fig. 5(b).

The curves for three records were compared for the contribution of uncertainties from various sources (Fig. 6). The index numbers of records shown in this figure refer to those of the ordinary ground motion records of FEMA P-695. The mean curves from Fig. 5(b) are also shown in Fig. 6 as the reference. The curves for “variable weights (8 samples)” are almost identical with those for “variable weights (16 samples)”, which indicates that 8 samples may be sufficient to consider the uncertainty of seismic weights. The curves for “fixed weights” typically match those for “variable weights” except in some local regions in Fig. 6(c). This result indicates that the uncertainty of seismic weights may not significantly affect the calculated conditional distributions of demand.

The optimized sample number of intensity measure depends on the targeted exceeding probability. For example, 40 samples appear to be sufficient for the CDF of 0.9 as 4 intensity samples fall in the tail of the curves even without the uncertainty of seismic weights (Fig. 5(a)). Other curves (Figs. 5 and 6) do not clearly show the number of intensity samples in the tail. Their optimized sample numbers can be justified to be the same with the fixed seismic weights based on the nature of MCS.

Lognormal distributions appear to fit the data very well in some instances (Figs. 6(a) and 6(b)) but not so well in others (Fig. 6(c)). This may be explained by the nature of IDA. The drift demand

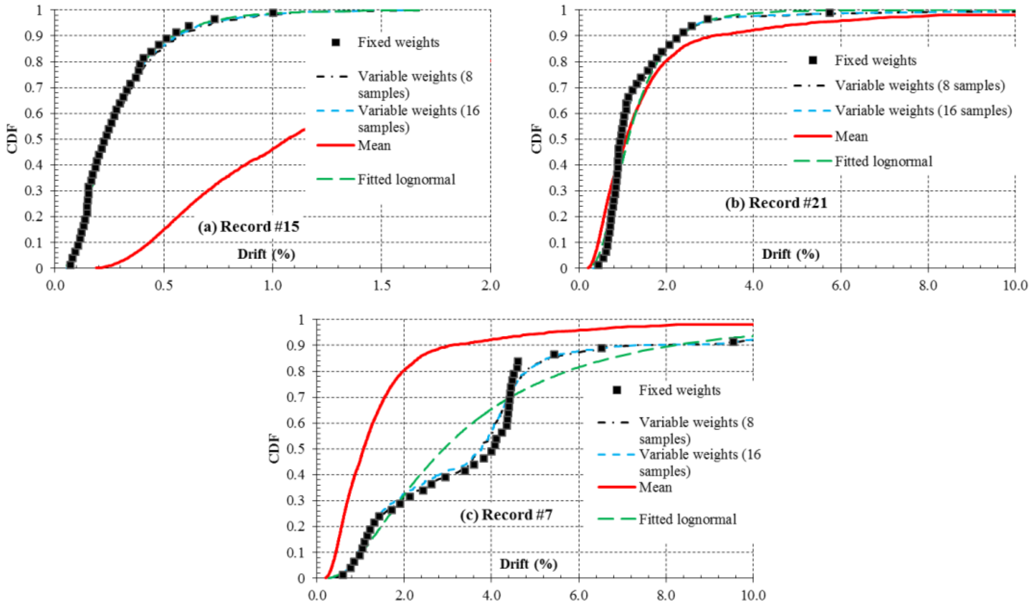

Fig. 6 Comparison of conditional distributions of three records for the second method

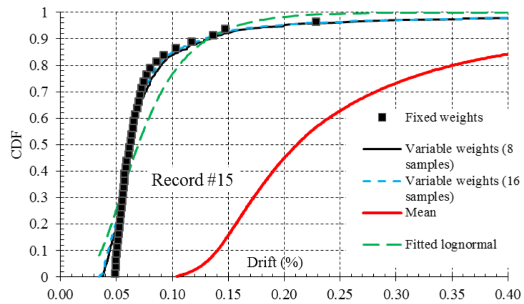

Fig. 7 Conditional distribution for the second method (the extreme-type distribution)

associated with Figs. 6(a) and 6(b) is close to a linear function of intensity measure while the intensity measure follows a lognormal distribution. When the nonlinearity between drift demand and intensity measure is significant, the lognormal distribution does not fit well (Fig. 6(c)). In order to further verify this explanation, the distribution of intensity measure was changed to the extreme-type as mentioned above. After the NTHA was performed, the results are shown in Fig. 7. Comparing these results with in Fig. 6(a), the lognormal distribution does not fit the data well in this case. A similar conclusion can be drawn from the comparison for other records. Therefore, the fitness of any distribution depends on several factors including the nature of IDA results and the assumed distribution types of the intensity measure and records.

5.3 Sensitivity analysis with the MCS method for the two-storey building

Three probability distribution curves are shown in Fig. 8. In this figure, the curve of “fixed weights (40 intensity samples)" was produced by ranking drift demand from 22 pairs of records scaled to 40 levels of spectral acceleration without the consideration of the uncertainty from seismic weights. Similarly, the curve of "fixed weight (10 intensity samples)" consists of 10 levels of spectral acceleration. The curve of "variable weights" was produced by ranking drift demand from 14080 samples.

From Fig. 8, it can be observed that three curves are almost identical regardless of their different sample sizes for intensity measure or the consideration of uncertainty from seismic weights. The agreement of three curves can be further observed from numerical calculation of drift demand at certain level of exceeding probability. The drift demand at 90% of exceeding probability from fixed seismic weights with 40 samples for intensity, fixed seismic weights with 10 samples for intensity and variable seismic weights are 3.13%, 3.14% and 3.12%, respectively (Table 2). This result confirms that the uncertainty of seismic weights does not significantly contribute to the overall distribution of drift demand, although seismic weights do affect some conditional distributions locally. The comparison from the "2nd lognormal" and extreme-type distributions shows a similar conclusion (Figs. 9 and 10). This result can be explained that the uncertainties from ground motion records and intensity measure dominate the variation of the resulting probability distribution of demand for the buildings studied in this paper. It is noted that a COV of 0.1 used for seismic weights is a reasonable estimation while a COV of 0.3 for intensity measure may have been underestimated. Therefore, the uncertainty of seismic weights may not need to be considered in typical seismic reliability analysis.

Figs. 8, 9 and 10 also indicate the optimized number of samples for intensity measure. If the region of interest for the CDF is near 0.9, 10 samples for intensity appear to be good enough to

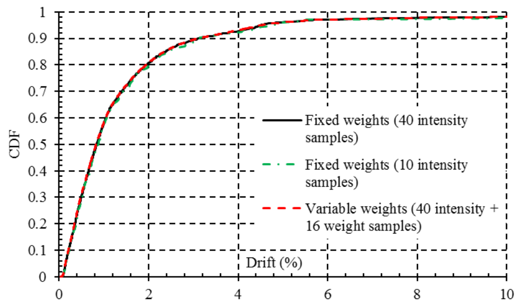

Fig. 8 Probability distribution from the MCS method

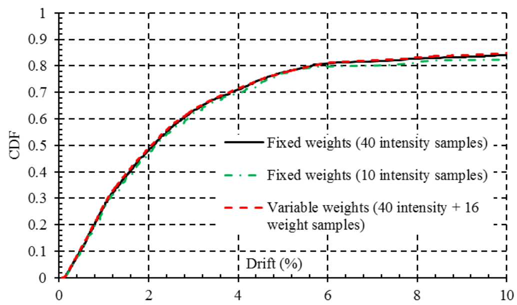

Fig. 9 Probability distribution from the MCS method (the 2nd lognormal distribution)

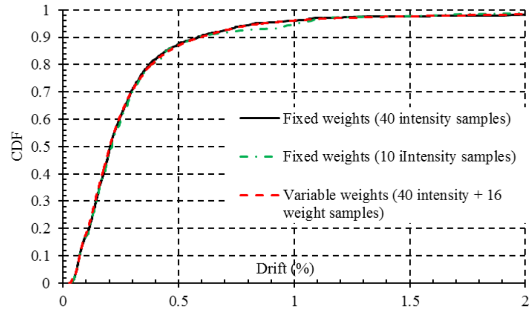

Fig. 10 Probability distribution from the MCS method (the extreme-type distribution)

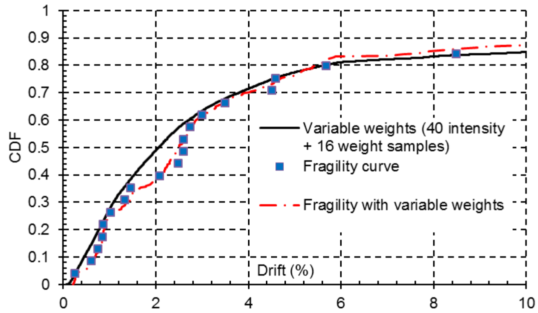

Fig. 11 Fragility curves from the MCS method (the 2nd lognormal distribution)

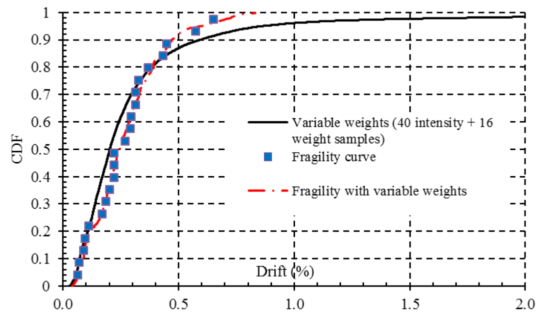

Fig. 12 Fragility curves from the MCS method (the extreme-type distribution)

provide a reasonable approximation. Using 40 samples for intensity measure does not measurably improve the accuracy of results for CDF=0.9. More samples for intensity measure will make the curves smoother and may be necessary if the design CDF approaches to its tail.

The probability distributions obtained from MCS may be used to calibrate the fragility analysis established at a fixed intensity level (Fig. 3). For comparison, the fixed intensity levels shown in Figs. 11 and 12 were chosen to be the mean value of their probability distributions. These two figures show the comparison for the second lognormal distribution and the extreme-type distribution, respectively. The figures also show another type of fragility curve with the uncertainties from both ground motion records and seismic weights, also known as “fragility with variable weights". The comparison shown in these figures further confirms that fragility curves without considering the variation from intensity may not accurately represent the probability distribution curves.

5.4 Comparison of different methods for the two-storey building

The exceeding probability (P_f) at given drift capacity levels can be computed with the three methods discussed above. With the traditional and second methods, the conditional distributions from IDA may have limited data points. A general way is to fit the data points with certain distributions, with which the exceeding probability can be computed. However, the error of the data fitting technique may be accumulated through the addition of multiple conditional distributions. The discrepancy of results observed in Tables 2, 3 and 4 may be partially explained by the error of data-fitting. In order to improve the accuracy for the traditional and second methods, linear interpolation can be used if the drift capacity is within the boundary of data points. The conditional distributions of "variable weights (16 samples)" shown in Fig. 4 were used as an example. A drift capacity of 7% has exceeded the value of the greatest drift demand (2%) of the curve in Fig. 4(a). Therefore, the fitted lognormal distribution had to be used. In Fig. 4(c), the same 7% drift capacity is within the range of the solid curve. Thus, the exceeding probability at the drift capacity of 7% can be determined from linear interpolation. The accuracy of the linear interpolation and data fitting can be observed from the difference between the curves shown in Fig. 4(c). As a comparison, the results of this lognormal distribution are shown in Table 3 while the results for the extreme-type distribution are shown in Table 4.

Table 2 Exceeding probability at 7% drift capacity and drift capacity at 10% exceeding probability for the lognormal distribution

	P_f @ 7% drift		Drift @ P_f = 10%	
	Partial data-fitting[1]	All data-fitting[2]	Partial data-fitting[1]	All data-fitting[2]
Traditional method	2.84%	3.38%	3.13%	3.30%
The 2nd method	2.63%	2.73%	3.14%	3.28%
MCS	2.57%		3.12%	

Note: [1]"Partial data-fitting" refers to that some results of conditional distributions are obtained from linear interpolation
[2]"All data-fitting" refers to that all results of conditional distributions are obtained from data-fitted lognormal distribution

Table 3 Exceeding probability at 7% drift capacity and drift capacity at 10% exceeding probability for the 2nd lognormal distribution

	P_f @ 7% drift		Drift @ P_f = 10%	
	Partial data-fitting	All data-fitting	Partial data-fitting	All data-fitting
Traditional method	18.0%	20.3%	18.6%	16.2%
The 2nd method	17.9%	21.2%	18.7%	14.6%
MCS	17.9%		20.1%	

Table 4 Exceeding probability at 7% drift capacity and drift capacity at 10% exceeding probability for the extreme-type distribution

	Pf @ 7% drift		Drift @ Pf= 10%	
	Partial data-fitting	All data-fitting	Partial data-fitting	All data-fitting
Traditional method	0.16%	0.19%	0.60%	0.60%
The 2nd method	0.16%	0.15%	0.59%	0.60%
MCS	0.14%		0.64%	

The results using the MCS shown in Tables 2-4 were considered to be relatively accurate. These results from the partial data-fitting (with linear interpolation) are close to those obtained from the MCS, which indicates that the partial data-fitting is more accurate than all data-fitting to produce the conditional distributions. The comparison of results also indicates that the traditional and second methods may slightly over-estimate the exceeding portability. This overestimation may be explained by the nature of the conditional distributions used by the traditional and second methods. At lower intensity levels, data-fitted conditional distributions always produce some values of probability of failure, the error from which is accumulated through the calculation.

5.5 Results of the four-storey apartment building and summary

The results of the four-storey building are very similar to those of the two-storey building. Examples of the results are shown in Fig. 13-15. These results confirms the findings that have been observed from the two-storey building as discussed above. The main sources of uncertainties of seismic demand comes from ground motion records and intensity measure. The variation of seismic weights does affect some conditional distributions for the traditional method and second method. A COV of 0.1 of seismic weights does not contribute much to the overall probability distributions of seismic demand. It does not appear to be necessary to consider the uncertainty from seismic weights with the MCS for both buildings studied in this paper.

If the uncertainty of seismic weights need to be considered for the traditional and second methods, eight samples may be sufficient to construct the conditional distribution curves. For the second method, the optimized sample number of intensity depends on the targeted exceeding

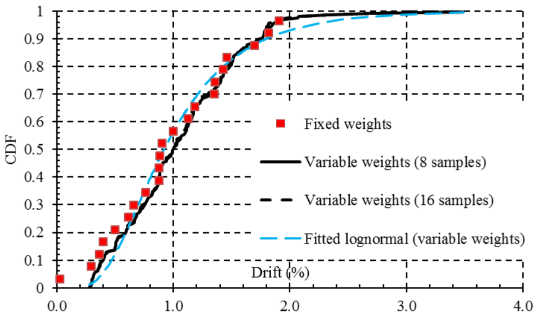

Fig. 13 Comparison of conditional probability distributions for the traditional method (4-storey building)

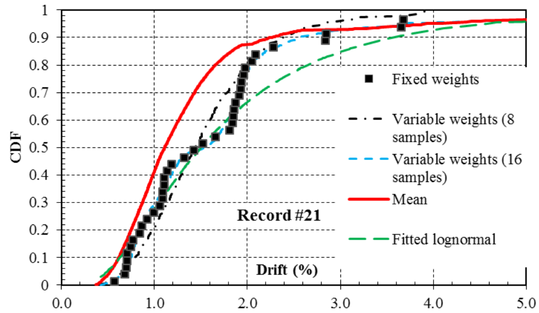

Fig. 14 Comparison of conditional distributions for the second method (4-storey building)

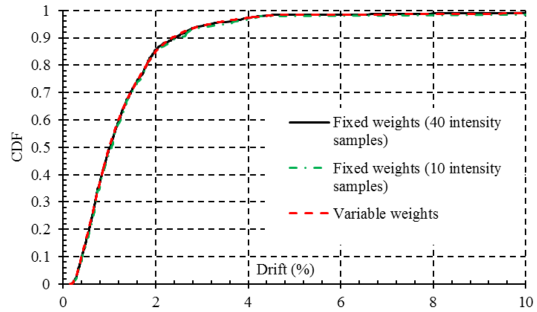

Fig. 15 Probability distribution from the MCS method (4-storey building)

probability. Forty (40) samples used in this analysis appear to produce satisfactory results. For the MCS method, 16 samples appear to produce satisfactory results for a COV of 0.3 even without the consideration of uncertainty from seismic weights.

The data-fitting using certain assumed distributions results the loss of some accuracy. For the traditional and second method, using data-fitting techniques to obtain conditional distributions causes some error, which may be accumulated to the final results. Whether a lognormal distribution can fit the data points well depends on several factors, including the nature of IDA results and the assumed distribution type of intensity measure and records. In order to improve the accuracy, the partial data-fitting with linear interpolation may be used if the targeting data are within the boundary of data points of the probability distributions.

6. Conclusions

Three seismic reliability methods and their corresponding numerical procedures were used for sensitivity analysis of wood frame structures. Two buildings were analyzed, including a two-storey house representing typical low-rise residential buildings and a four-storey apartment building representing typical multi-storey construction. Two types of probability distributions for intensity measure were used: the lognormal distribution and the extreme-type distribution. The sources of uncertainties include ground motion records, intensity measure and seismic weights. Different sample numbers were used to study the marginal contributions of related factors.

The results of sensitivity analysis show that the main sources of uncertainties come from ground motion records and intensity measure. Seismic weights do not appear to contribute much to the overall probability distribution of the seismic demand of the buildings. If the uncertainty of seismic weights has to be considered in conditional distributions, eight samples may be sufficient. The sample number for intensity measure used by the second method depends on the targeted exceeding probability. Forty samples appear to be sufficient for a COV of 0.3. With the MCS, 16 samples for intensity measure appear to be enough. When data-fitted conditional distributions are used in the traditional and second methods, the error from data-fitting techniques may be accumulated through the calculation. In order to improve the accuracy of results, linear interpolation combined with data-fitted distributions can be used to compute the conditional distributions. The results of probability failure are found to heavily depend on the probability distribution types of intensity used in the analysis, as well as the drift capacity. The methods and results in this paper will provide a benchmark to quantify the safety margin of such wood buildings under earthquake loadings, if a proper probability distribution of intensity and the ultimate drift capacity under extreme loadings can be defined.

References

Applied Technology Council (ATC) (2009), "Quantification of building seismic performance factors", FEMA P-695 report, Federal Emergency Management Agency (FEMA), U.S. Department of Homeland Security, Washington, DC.

Ceccotti, A. and Foschi, R.O. (1999), "Reliability assessment of wood shear walls under earthquake excitation", *Proceedings of the 3rd International Conference on Computational Stochastic Mechanics*, Balkema, Brookfield, Vermont.

Cornell, C.A., Jalayer, F., Hamburger, R.O. and Foutch, D.A. (2002), "Probabilistic basis for 2000 SAC Federal Emergency Management Agency steel moment frame guidelines", *J. Struct. Eng.*, **128**(4), 526-533.

Ellingwood, B., Rosowsky, D., Li, Y. and Kim, J. (2004), "Fragility assessment of light-frame wood construction subjected to wind and earthquake hazards", *J. Struct. Eng.*, **130**(12), 1921-1930.

Filiatrault, A., Christovasilis, I., Wanitkorkul, A. and van de Lindt, J. (2010), "Experimental seismic response of a full-scale light-frame wood building", *J. Struct. Eng.*, **136**(3), 246-254.

Filiatrault, A. and Folz, B. (2002), "Performance-based seismic design of wood framed buildings", *J. Struct. Eng.*, **128**(1), 39-47.

Fischer, D., Filiatrault, A., Folz, B., Uang, C.M. and Seible, F. (2001), "Shake table tests of a two-story woodframe house", CUREE Rep. No. W-06, Task 1.1.1, Consortium of Universities for Research in Earthquake Engineering, Richmond, California.

Folz, B. and Filiatrault, A. (2001), "Cyclic analysis of wood shear walls", *J. Struct. Eng.*, **127**(4), 433-441.

Folz, B. and Filiatrault, A. (2004), "Seismic analysis of woodframe structures II: model implementation and verification", *J. Struct. Eng.*, **130**(9), 1361-1370.

Li, Y., Yin, Y., Ellingwood, B.R. and Bulleit, W.M. (2010), "Uniform hazard versus uniform risk bases for performance-based earthquake engineering of light-frame wood construction", *Earthq. Eng. Struct. Dyn.*, **39**(11), 1199-1217.

Pang, W., Rosowsky, D.V., Ellingwood, B.R. and Wang Y. (2009), "Seismic fragility analysis and retrofit of conventional residential wood-frame structures in the Central United States", *J. Struct. Eng.*, **135**(3), 262-271.

Pei, S., van de Lindt, J. and Popovski, M. (2012), "Approximate R-factor for cross laminated timber walls in multi-story buildings", *J. Archit. Eng.*, **19**(4), 245-255.

Rosowsky, D.V. (2002), "Reliability-based seismic design of wood shear wall", *J. Struct. Eng.*, **128**(11),

1439-1453.
Vamvatsikos, D. and Cornell, C.A. (2002), "Incremental dynamic analysis", *Earthq. Eng. Struct. Dyn.*, **31**(3), 491-514.
van de Lindt, J., Pei, S., Pryor, S.E., Shimizu, H. and Isoda, H. (2010), "Experimental seismic response of a full-scale six-story light-frame wood building", *J. Struct. Eng.*, **136**(10), 1262-1272.
van de Lindt, J., Rosowsky, D., Pang, W. and Pei, S. (2013), "Performance-based seismic design of midrise woodframe buildings", *J. Struct. Eng.*, **139**(8), 1294-1302.
Wang, C.H. and Foliente, G.C. (2006), "Seismic reliability of low-rise nonsymmetric woodframe buildings", *J. Struct. Eng.*, **132**(5), 733-744.
Zhang, J. and Foschi, R.O. (2004), "Performance-based design and seismic reliability analysis using designed experiments and neural networks", *Prob. Eng. Mech.*, **19**(3), 259-267.

NM